Neurological Sciences
https://doi.org/10.1007/s10072-021-05704-2

ORIGINAL ARTICLE

Cerebral amyloid load determination in a clinical setting: interpretation of amyloid biomarker discordances aided by tau and neurodegeneration measurements

Matilde Nerattini[1] · Federica Rubino[1] · Annachiara Arnone[1] · Cristina Polito[2] · Salvatore Mazzeo[2] · Gemma Lombardi[3] · Giulia Puccini[4] · Benedetta Nacmias[2,3] · Maria Teresa De Cristofaro[1] · Sandro Sorbi[2,3] · Alberto Pupi[1] · Roberto Sciagrà[1] · Valentina Bessi[2] · Valentina Berti[1]

Received: 21 June 2021 / Accepted: 26 October 2021

Abstract

Background Alzheimer's disease (AD) diagnosis can be hindered by amyloid biomarkers discordances.

Objective We aim to interpret discordances between amyloid positron emission tomography (Amy-PET) and cerebrospinal fluid (CSF) ($A\beta_{42}$ and $A\beta_{42/40}$), using Amy-PET semiquantitative analysis, [^{18}F]fluorodeoxyglucose (FDG)-PET pattern, and CSF assays.

Method Thirty-six subjects with dementia or mild cognitive impairment, assessed by neuropsychological tests, structural and functional imaging, and CSF assays ($A\beta_{42}$, $A\beta_{42/40}$, p-tau, t-tau), were retrospectively examined. Amy-PET and FDG-PET scans were analyzed by visual assessment and voxel-based analysis. SUVR were calculated on Amy-PET scans.

Results Groups were defined basing on the agreement among CSF $A\beta_{42}$ (A), CSF $A\beta_{42/40}$ Ratio (R), and Amy-PET (P) dichotomic results (±). In discordant groups, CSF assays, Amy-PET semiquantification, and FDG-PET patterns supported the diagnosis suggested by any two agreeing amyloid biomarkers. In groups with discordant CSF $A\beta_{42}$, the ratio always agrees with Amy-PET results, solving both false-negative and false-positive $A\beta_{42}$ results, with $A\beta_{42}$ levels close to the cut-off in A + R-P- subjects. The A + R + P- group presented high amyloid deposition in relevant areas, such as precuneus, posterior cingulate cortex (PCC) and dorsolateral frontal inferior cortex at semiquantitative analysis.

Conclusion The amyloid discordant cases could be overcome by combining CSF $A\beta_{42}$, CSF ratio, and Amy-PET results. The concordance of any 2 out of the 3 biomarkers seems to reveal the remaining one as a false result. A cut-off point review could avoid CSF $A\beta_{42}$ false-negative results. The regional semiquantitative Amy-PET analysis in AD areas, such as precuneus and PCC, could increase the accuracy in AD diagnosis.

Keywords Alzheimer's disease · Plaque, Amyloid · Positron emission tomography · Cerebrospinal fluid · Biomarkers

Introduction

In an effort to improve Alzheimer's disease (AD) diagnostic accuracy, the National Institute on Aging and the Alzheimer's Association (NIA-AA) workgroup's research framework has recently proposed the AT(N) biomarker algorithm, consisting in a descriptive classification scheme based on the features of AD biomarkers. In the AT(N) system, the "A" category includes biomarkers of β amyloid (Aβ) deposition, the "T" parameter stands for neurofibrillary tangles, and "N" represents the extent of neurodegeneration [1]. Each of those can be evaluated using either cerebrospinal fluid (CSF) measurements or magnetic resonance (MRI) and positron emission tomography (PET) imaging.

✉ Matilde Nerattini
matilde.nerattini@unifi.it

1 Nuclear Medicine Unit, Azienda Ospedaliero-Universitaria Careggi, Largo Piero Palagi 1, 50139 Florence, Italy

2 Department of Neuroscience, Psychology, Drug Research and Child Health, University of Florence (NEUROFARBA), Azienda Ospedaliero-Universitaria Careggi, Largo Brambilla 3, 50134 Florence, Italy

3 IRCCS Fondazione Don Carlo Gnocchi, Via Scandicci 269, 50143 Florence, Italy

4 Department of Nuclear Medicine, Hospital of Prato, Via Suor Niccolina Infermiera, 20/22, 59100 Prato, Italy

Published online: 05 November 2021

In particular, the biomarkers of Aβ plaque deposits include Aβ 1–42 levels ($Aβ_{42}$) in CSF and ligand retention on PET with radiopharmaceuticals for Aβ (Amy-PET) [2]. Regarding the pathophysiological process, it has been known that CSF $Aβ_{42}$ levels correlate inversely with brain amyloid plaque load and decrease early in the disease process [3] while Amy-PET imaging provides a more direct information on brain amyloid load at a specific moment of the disease process [4] with diagnostic sensitivity and specificity of 96–98% and 89–100%, respectively [5]. Amy-PET and CSF $Aβ_{42}$ have been included as interchangeable diagnostic tools for both research [1, 6, 7] and clinical practice [8, 9]. Nevertheless, discordant results can occur, representing one of the major limits to an accurate and early diagnosis of AD [6, 8, 9]. In literature, the percentage of Aβ discordant cases is about 10–20% in both normal elderly and patients [10, 11]. Many studies have suggested that CSF $Aβ_{42}$ levels decrease before the fibrillar $Aβ_{42}$ deposition becomes detectable by Amy-PET [4, 12], although some works supported the opposite [13]. It should be noted that while PET tracers directly bind to brain fibrillar Aβ, CSF analysis provides levels of soluble Aβ, identifying a pathologic condition less strictly associated with the amyloid plaque formation [1]. On one hand, this fact could justify the different timing in amyloid biomarker alteration; on the other hand, it has led to hypothesize that the two biomarkers could provide partly independent information on amyloid pathology [14]. The variability in individual Aβ metabolism could be another possible explanation for discordance [15]: the addition of CSF $Aβ_{42/40}$ ratio (R) to the available panel of biomarkers can be helpful in correctly identifying patients with AD [16]. $Aβ_{42/40}$ R has been shown to minimize the number of discordant cases by normalizing CSF $Aβ_{42}$ concentration to the level of the most abundant cerebral Aβ isoform (Aβ 1–40) [17, 18]; however, still controversy exists. Moreover, it has been observed that CSF $Aβ_{42}$ levels are also reduced in other non-AD conditions, including Creutzfeldt-Jakob's disease, amyotrophic lateral sclerosis, and neuroinflammation [19]. Finally, the CSF cut-off choice could influence biomarker determination, representing a common limitation suggested by several studies [1, 20]. The main advantages of Amy-PET are the minimal invasiveness and the possibility of cerebral regional evaluation, which could give also a grading of amyloid deposition. Semiquantitative analyses such as standardized uptake value ratio (SUVR) are used to improve visual interpretation and the overall accuracy in estimating amyloid plaque distribution within distinct brain regions [21]. However, even in this case, there is not yet a universally accepted threshold value to define Aβ positivity [22].

Using a sample of cognitively impaired subjects derived from clinical practice, our real-life study takes part in the well-known debate about discordance between CSF $Aβ_{42}$ and Amy-PET as biomarkers of amyloid pathology. Unlike interclass biomarker incongruence, no explicit recommendations have been suggested in cases of incongruous results within the same intraclass biomarkers [8]. Our aim is to improve the interpretation of discordant cases by integrating the data extracted from both Amy-PET and CSF ($Aβ_{42}$ and R) examinations, supported by semiquantitative and voxel-based analysis of Amy-PET results, and by measurements of T and N parameters, using FDG-PET metabolic patterns and CSF assays.

Materials and methods

Subjects

Thirty-six subjects were extracted from a single-center retrospective observational study carried out at the University of Florence between 2017 and 2019 and partially overlap with a previous study [23]. The criteria for retrospective inclusion were as follows: (1) dementia or mild cognitive impairment (MCI) due to AD as possible diagnoses, according to current diagnostic criteria [8, 9], and (2) extensive diagnostic workup already performed as part of clinical routine, including neuropsychological tests, ApoE genotype determination, brain CT/MRI, FDG-PET scan, Amy-PET scan, and CSF sampling. The exclusion criteria were (1) presence of secondary causes of cognitive decline (e.g., normal pressure hydrocephalus, subdural hematoma, brain tumor or stroke at the cognitive symptoms onset, or the presence of a relevant vascular injury on the brain CT/MRI (Fazekas score above 2) [24, 25].

Participants (or their caregivers) gave informed consent for all investigations, and study procedures were approved by the local Institutional Review Board (reference 15691_oss).

CSF acquisition and analysis

CSF samples were stored at – 80 °C until the moment of the analysis that was performed in a single batch with the automated Fujirebio Lumipulse system [26], utilizing one single kit. The cut-off values for CSF $Aβ_{42}$, CSF $Aβ_{42/40}$, CSF p-tau, and CSF t-tau were determined following Fujirebio guidelines for the chemiluminescent enzyme immunoassay (CLEIA) Lumipulse method (diagnostic sensitivity and specificity using clinical diagnosis and follow-up gold standard. November 19, 2018).

Each CSF measurement was classified as positive for AD according to validated cut-off values as follows: CSF $Aβ_{42} < 874$ pg/ml, CSF AβR < 0.1, CFS p-tau > 61 pg/ml, CSF t-tau > 400 pg/ml [26].

PET acquisition and processing

Amy-PET scans were performed with any of the ^{18}F-labeled radiotracers commercially available.

The injection and the image acquisition were executed following the current guidelines for each radiotracer:

- 300 MBq Florbetaben (FBB)-Bayer-Piramal, image acquisition after 90 min
- 185 MBq Flutemetamol (FMM)-General Electric, image acquisition after 90 min

For FDG-PET scans, image acquisition was performed 30–40 min after ^{18}F-FDG administration (3.7 MBq/kg), according to EANM guidelines for brain imaging.

Both Amy-PET and FDG-PET images were obtained on a PET/CT scanner (Philips Gemini TF 16 PET/CT), and reconstructions were performed using 3D LOR iterative algorithm reconstruction (FOV, 256; matrix, 128 × 128; voxel dimensions, 2 × 2 × 2 mm). CT acquisitions for attenuation correction were performed on spiral 16 slices CT with a slice thickness of 2 mm.

For Amy-PET, a binary positive/negative output was established by certified readers in a consensus reading based on visual assessment.

SPM and ROI analysis

FDG PET data were analyzed using statistical parametric mapping (SPM12) [27] on MATLAB (MathWorks Inc, Sherborn, MA, USA). Scans were manually reoriented, setting the origin to the anterior commissure, normalized to dementia-specific [^{18}F]-FDG-PET template [28, 29], and then smoothed (FWHM 8 mm). Comparisons between groups were performed using ANOVA design, including a group of controls provided by AIMN with age as nuisance variable. The significance threshold was set at $p < 0.05$, FWE-corrected for multiple comparisons at the voxel level. Only clusters containing more than 16 voxels were deemed to be significant.

Amy-PET data were analyzed using SPM12 [27] on MATLAB (MathWorks Inc, Sherborn, MA, USA). Image scans were manually reoriented, setting the origin to the anterior commissure, normalized to TPM template, and then smoothed (FWHM 8 mm). Comparisons between groups were performed using ANOVA analysis, with age as nuisance variable and proportional scaling to cerebellar GM uptake. The significance threshold was set at $p < 0.05$, FWE-corrected for multiple comparisons at the voxel level. Only clusters containing more than 16 voxels were deemed to be significant.

ROI analyses were conducted on Amy-PET scans. We chose all ROIs obtained by the automated anatomical labeling 3 (AAL3) atlas [30] to extract regional uptake from normalized Amy-PET. ROIs were created using Pickatlas tool, and amyloid tracer uptake values were extracted using MarsBar tool. Then, SUVR values were calculated using the cerebellar GM as reference and standardized with each other.

Statistical analysis

All statistical analyses have been performed with software IBM® SPSS® Statistics. Comparisons between variables have been performed using chi-square test or ANOVA univariate, with LSD method for post hoc analyses, as appropriate. Statistical significance was set at $p < 0.05$.

Results

Participants

Participants' characteristics are shown in Table 1.

Table 1 *Demographic and clinical characteristics, cerebrospinal fluid features, and global SUVR values of groups.* Groups were formed considering CSF $A\beta_{1\text{-}42}$ (A), CSF $A\beta_{42/40}$ ratio (R), and Amy-PET (P) dichotomic evaluations (±). Cut-off for normal values: CSF $A\beta_{42} > 874$ pg/ml, CSF AβR > 0.1, CFS p-Tau < 61 pg/ml, CSF t-tau < 400 pg/ml. Abbreviations: *MMSE* Mini-Mental State Examination; *p-tau* phosphorylated tau; *t-tau* total tau; *SUVR* standardized uptake value ratio; *CSF* cerebrospinal fluid

	A + R + P +	A-R + P +	A + R + P-	A + R-P-	A-R-P-
No. of subjects	21 (58.3%)	3 (8.3%)	6 (16.6%)	3 (8.3%)	3 (8.3%)
Age	64 ± 7	70 ± 5	75 ± 5	58 ± 7	68 ± 3
Sex (% F)	70%	67%	50%	67%	0%
MMSE	20 ± 5	24 ± 1	20 ± 5	23 ± 5	24 ± 1
$A\beta_{1\text{-}42}$	522 ± 161	1002 ± 87	463 ± 238	769 56	1193 ± 206
$A\beta_{1\text{-}42/1\text{–}40}$	0.06 ± 0.01	0.06 ± 0.01	0.06 ± 0.01	0.13 ± 0.01	0.14 ± 0.01
p-tau	105 ± 42	141 ± 16	131 ± 48	24 ± 7	47 ± 19
t-tau	677 ± 266	848 ± 68	781 ± 273	258 ± 151	360 ± 106
Global SUVR	1.53 ± 0.17	1.52 ± 0.03	1.28 ± 0.23	1.11 ± 0.16	1.01 ± 0.07

According to the dichotomic evaluation (±) of CSF $A\beta_{42}$ (A), CSF $A\beta_{42/40}$ ratio (R), and Amy-PET scans (P), patients were grouped pursuant to the concordance (positivity or negativity), of all 3 methods (concordants' groups) or to the concordance of 2 out of 3 methods (discordants' groups). Since none of the subject fell in the A-R + P-, A-R-P +, or A + R-P + groups, overall the patients resulted to be distributed into five groups: A + R + P +, A-R-P-, A + R + P-, A + R-P-, and A-R + P +.

There are no significant differences between groups in MMSE, age, and sex distribution.

Concordance among amyloid biomarkers

Groups' CSF $A\beta_{42}$ and $A\beta_{42/40}$ mean values and global SUVR are shown in Table 1.

A + R + P + group (triple-positive, 58.3%) presented CSF p-tau and t-tau values indicative for tau-pathology and neurodegeneration, respectively. FDG-PET demonstrated significant hypometabolism in several cortical regions including parietal-temporal lobes and precuneus (Fig. 1, Table 2).

A-R-P- group (triple-negative, 8.3%) presented CSF p-tau and t-tau values under the cut-off. FDG-PET scans did not show statistically significant hypometabolism.

Discordance among amyloid biomarkers

Groups' CSF $A\beta_{42}$ and $A\beta_{42/40}$ mean values and global SUVR are shown in Table 1.

A + R + P- group (16.6%) presented CSF p-tau mean value indicative of tau-pathology. Considering neurodegeneration, CSF t-tau was above the cut-off and FDG-PET

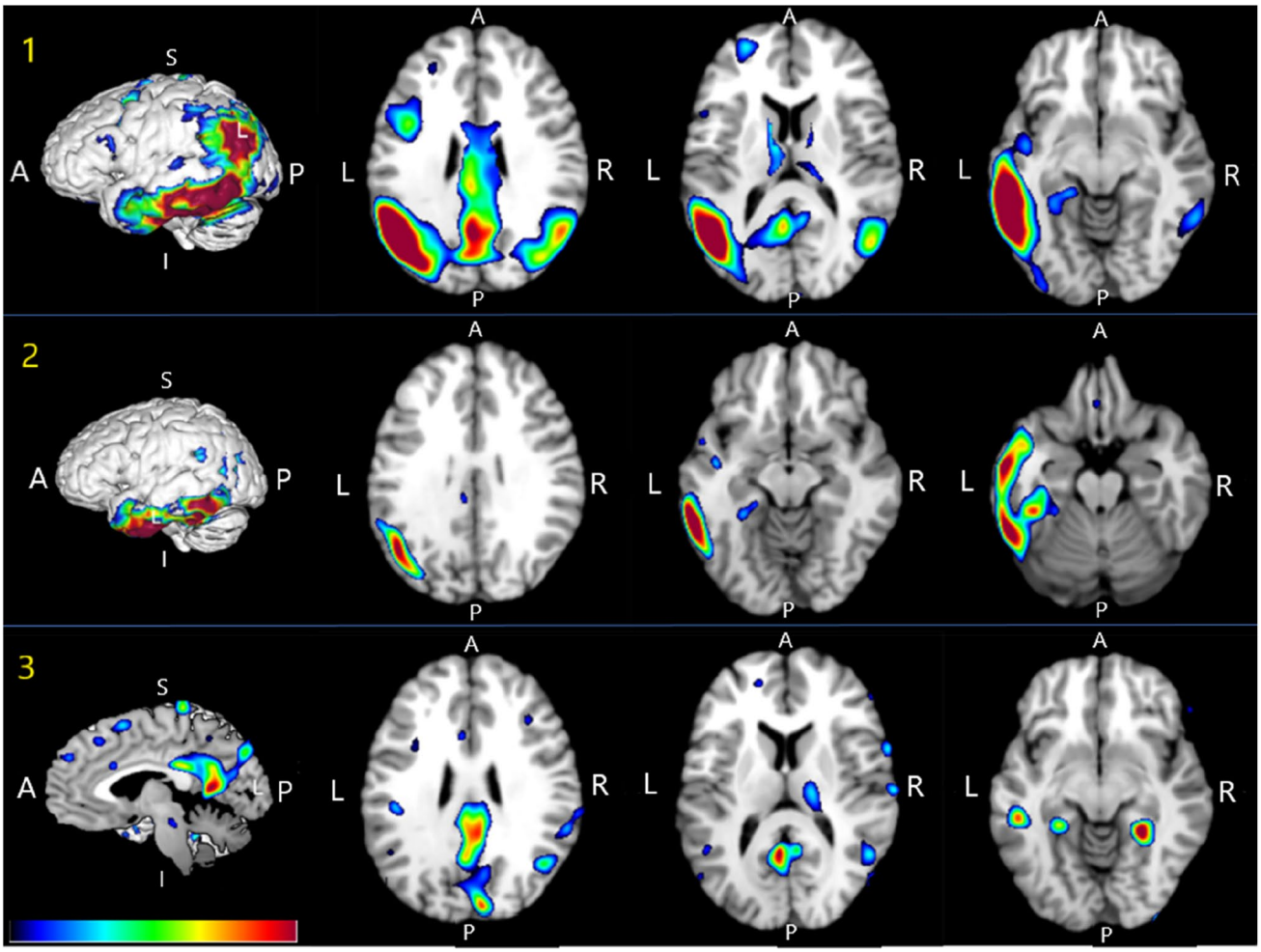

Fig.1 Statistical Parametric Maps (SPMs) showing significant regional FDG-hypometabolism in the A + R + P + (Panel 1), A + R + P- (Panel 2) and A-R + P + (Panel 3) groups, compared to the AIMN healthy controls dataset. SPMs are represented on color-coded scale and displayed onto a standardized MRI. All the results are shown at $p < 0.05$, FWE corrected for multiple comparisons at the voxel level and adjusted for age. Corresponding coordinates and anatomical areas can be found in Table 2. Abbreviations: L, left; R, right; A, anterior; P, posterior; S, superior; I, inferior; FDG, [^{18}F]-Fluorodeoxyglucose; AIMN, Associazione Italiana Medicina Nucleare; MRI, magnetic Resonance Imaging

Table 2 *Brain regions showing significant regional FDG-PET hypometabolism in the A(x)R(x)P(x) groups, compared to the AIMN healthy controls dataset.* * *T* and *Z* values are extracted at the peak of maximum significance at $p < 0.05$, correcting for age. Only contrasts yielding significant results are reported. † coordinates (x, y, z) are from Talairach and Tournoux. Abbreviations: *A*, cerebrospinal fluid amyloid β 1–42; *R*, cerebrospinal fluid amyloid β 1–42/1–40; *P*, amyloid positron emission tomography; *AIMN* Associazione Italiana Medicina Nucleare; *HC* health controls; *FDG* [^{18}F]-Fluorodeoxyglucose; *PET* positron emission tomography

Cluster extent	T *	Z *	x, y, z †	Anatomical region	Brodmann area
A + R + P + < AIMN-HC					
7117	10.36	Inf	− 41, − 48, 46	Left cerebrum, parietal lobe, inferior parietal lobule	40
	9.92	Inf	− 49, − 53, 36	Left cerebrum, parietal lobe, inferior parietal lobule	40
	9.80	Inf	− 59, − 49, 0	Left cerebrum, temporal lobe, middle temporal gyrus	21
708	6.61	6.24	− 4, − 51, 34	Left cerebrum, parietal lobe, precuneus	7
	5.79	5.53	− 4, − 64, 39	Left cerebrum, parietal lobe, precuneus	7
	5.00	4.82	8, − 46, 27	Right cerebrum, parietal lobe, precuneus	31
444	5.65	5.41	41, − 58, 45	Right cerebrum, parietal lobe, inferior parietal lobule	40
	5.59	5.36	47, − 46, 45	Right cerebrum, parietal lobe, inferior parietal lobule	40
	5.33	5.13	53, − 51, 34	Right cerebrum, parietal lobe, supramarginal gyrus	40
17	5.04	4.87	− 43, 12, 40	Left cerebrum, frontal lobe, middle frontal gyrus	8
20	5.04	4.86	59, − 45, − 10	Right cerebrum, temporal lobe, inferior temporal gyrus	20
A + R + P- < AIMN-HC					
4428	7.76	7.19	− 43, − 41, − 13	Left cerebrum, temporal lobe, fusiform gyrus	37
	7.68	7.12	− 55, − 17, − 21	Left cerebrum, temporal lobe, fusiform gyrus	20
	7.08	6.63	− 61, − 44, − 2	Left cerebrum, temporal lobe, middle temporal gyrus	21
101	5.66	5.42	− 10, 17, − 3	Left cerebrum, sub-lobar, caudate	Caudate head
16	5.10	4.92	− 63, − 39, 26	Left cerebrum, parietal lobe, inferior parietal lobule	40
A-R + P + < AIMN-HC					
44	4.00	3.89	25, − 43, − 4	Right cerebrum, limbic lobe, parahippocampal gyrus	19
37	3.62	3.54	− 3, − 56, 19	Left cerebrum, limbic lobe, posterior cingulate	23
21	3.32	3.25	5, − 25, 24	Right cerebrum, limbic lobe, cingulate gyrus	23

scans showed hypometabolism in the middle temporal gyrus, fusiform gyrus, caudate head, and inferior parietal lobule (Fig. 1, Table 2).

A + R-P- group (8.3%) presented CSF p-tau mean value below the cut-off and significantly lower than A + R + P + and A + R + P- ones. CSF t-tau was in the normal range and FDG-PET scans did not show statistically significant hypometabolism.

A-R + P + group (8.3%) presented p-tau and t-tau values above the cut-off. FDG-PET scans showed hypometabolism in the parahippocampal gyrus, posterior cingulate, and cingulate gyrus (Fig. 1, Table 2).

Comparison of Aβ biomarkers between groups

Regarding CSF $A\beta_{42}$, concordant groups (A + R + P + and A-R-P-) showed opposite mean values, with a significant difference between each other. The mean A value was significantly lower in triple-positive vs A + R-P- and A-R + P +, whereas it was significantly higher in triple-negative vs A + R + P-. In discordant groups, A + R + P- and A + R-P- presented levels below the cut-off, with $A\beta_{42}$ average values in A + R + P- significantly lower than in A + R-P-. The $A\beta_{42}$ value in A + R + P- did not show a statistical difference vs triple-positive, and $A\beta_{42}$ levels in A + R-P- did not show a statistical difference versus $A\beta_{42}$ negatives groups (A-R + P + and A-R-P-). A-R + P + had $A\beta_{42}$ levels above the cut-off, with no significant difference as compared to triple-negative, neither to A + R-P-. (Fig. 2).

Moving to the ratio, discordant groups with a positive R (A + R + P- and A-R + P +) presented identical mean value, even equal to the triple-positives' one and significantly lower than A + R-P-. R in A + R-P- was close to A-R-P- one (not statistically different), and both of them showed significant differences vs A + R + P +, A + R + P- and A-R + P + (Fig. 2).

Focusing on Amy-PET semiquantitative analysis, SUVR values decrease from A + R + P + to A-R + P + to A + R + P- to A + R-P- to A-R-P-. In discordant groups, SUVR was significantly higher in A-R + P + vs A + R + P- and A + R-P- both globally and in the majority of brain regions: parietal lobe, temporal lobe, frontal lobe, insula, orbitofrontal cortex, medial frontal cortex, lateral temporal cortex, medial temporal cortex, lateral parietal cortex, and caudate head. The precuneus showed the same statistical differences, except for the comparison between

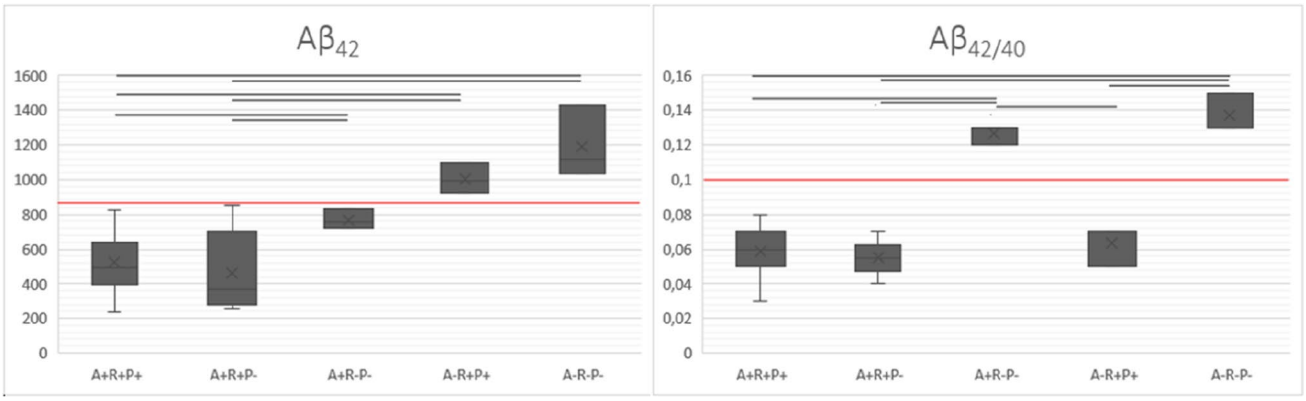

Fig.2 Comparing cerebrospinal fluid (CSF) $A\beta_{42}$ and $A\beta_{42/40}$ measurements across groups. Boxplots represent results of comparison analyses among groups regarding both $A\beta_{42}$ (pg/mL) and $A\beta_{42/40}$. Red lines correspond to cut-off values (874 pg/mL for $A\beta_{42}$ and 0,1 for the ratio). The lines in the upper part of the scheme show where differences among groups are statistically significant ($p < 0.05$). Abbreviations: A, cerebrospinal fluid amyloid β 1–42; R, cerebrospinal fluid amyloid β 1–42/ 1–40; P, amyloid positron emission tomography

A-R + P + and A + R + P- which did not show a significant difference. The posterior cingulate cortex (PCC) and the dorsolateral inferior frontal cortex in group A + R + P- presented mean values closer to Amy-PET positive subjects, with no statistical difference versus A + R + P + and A-R + P + (Fig. 3).

In Amy-PET voxel-based analysis, the amyloid deposition levels in the A-R + P + group resulted significantly higher than controls in the middle frontal gyrus, orbital gyrus, cingulate gyrus, caudate, and inferior parietal lobule (Fig. 4, Table 3). A + R + P + group showed brain amyloid deposits significantly higher than A-R-P- in the whole gray matter sparing occipital lobes, with a stronger significance and larger cluster extension in the precuneus, cingulate gyrus, and orbitofrontal cortex (Fig. 4, Table 3).

Discussion

Amyloid pathology in AD can be reliably detected with both CSF $A\beta_{42}$ measurements and Amy-PET scans [1] The accuracy of these different methods is demonstrated in many studies, confirming the prevalent agreement between the two types of amyloid biomarkers [12, 31]. This real-life study aimed to improve the interpretation of discordant cases by integrating the data extracted from both Amy-PET and CSF ($A\beta_{42}$ and R) examinations with the support of semiquantitative and voxel-based analysis of Amy-PET results, and with measurements of T and N parameters, using CSF assays and FDG-PET metabolic patterns. The relevant role of FDG-PET scans in supporting the diagnosis of dementing neurodegenerative disorders has been recently defined by the Delphi consensus [32].

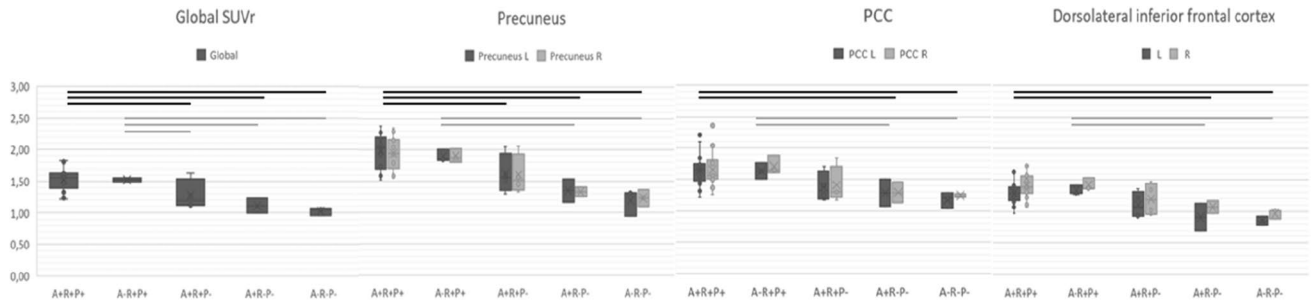

Fig.3 Comparing global and regional Standardized Uptake Value ratio (SUVr) across groups. Boxplots represent SUVr analysis results in global cerebrum and in crucial areas as precuneus, posterior cingulate gyrus and dorsolateral inferior frontal cortex. The lines in the upper part of the scheme show where differences among groups are statistically significant both in right (R) and left (L) cerebrum ($p < 0.05$). It is recognizable a SUVr characteristic decreasing pattern with progressively lower values from A + R + P + , to A-R + P + , to A + R + P-, to A + R-P-, to A-R-P-. Abbreviations: A, cerebrospinal fluid amyloid β 1–42; R, cerebrospinal fluid amyloid β 1–42/ 1–40; P, amyloid positron emission tomography; PCC, posterior cingulate gyrus; L, left; R, right

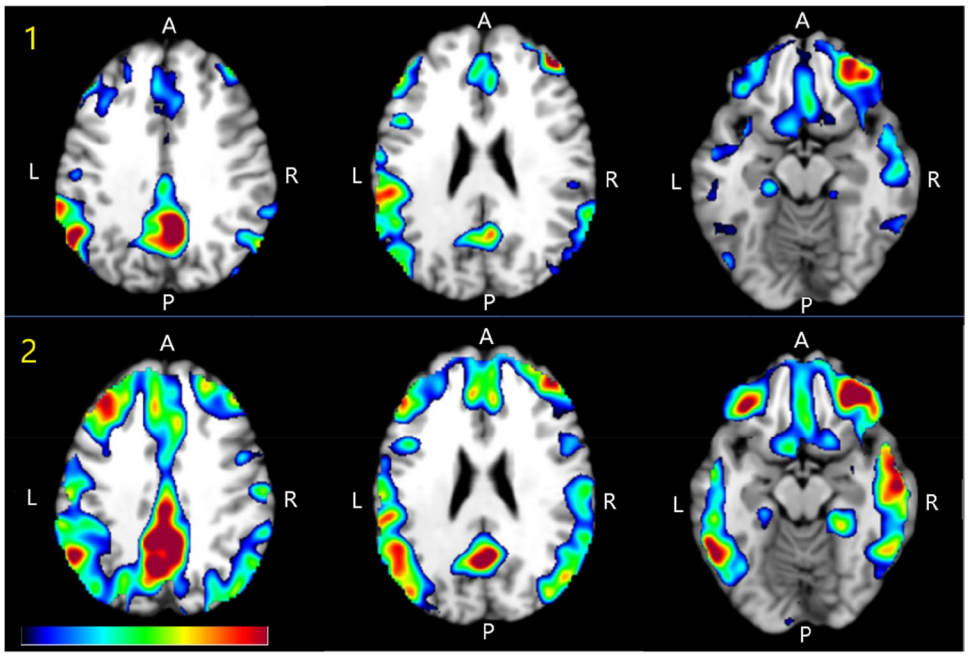

Fig.4 Statistical Parametric Maps (SPMs) showing high significant ^{18}F-labeled amyloid tracers' retention in A-R + P + (Panel 1) and A + R + P + (Panel 2) groups compared to controls (triple-negative subjects). SPMs are represented on color-coded scale and displayed onto a standardized MRI. All the results are shown at $p < 0.05$, FWE corrected for multiple comparisons at the voxel level and adjusted for age. Corresponding coordinates and anatomical areas can be found in Table 3. Abbreviations: L, left; R, right; A, anterior; P, posterior; MRI, magnetic Resonance Imaging

In line with literature, our results showed a high prevalence of concordance between Amy-PET and CSF $A\beta_{42}$ results (67%). As expected, in triple-positive subjects, all biomarkers suggested amyloid pathology due to AD. Amy-PET voxel-based analyses showed a widespread distribution of radiotracer in gray matter, which by definition characterizes an exam consistent with amyloid pathology [33]. It is interesting to notice the sparing of occipital lobes and the stronger significance and larger cluster extension in precuneus, cingulate gyrus, and orbitofrontal cortex than in the others regions investigated. These results are in line with the spatial pattern of amyloid plaque deposition in AD, first defined by Braak and Braak [34], with an early involvement of the orbitofrontal cortex and delayed amyloid deposition in occipital regions. Moreover, Palmqvist et al. showed recently how the early accumulation of β-amyloid occurs within the default mode network, starting preferentially in the medial orbitofrontal cortex, precuneus, and PCC [35]. In the semiquantitative analysis, we obtained for triple-positive subjects the highest global and regional SUVr values of the study, supporting high concentration of amyloid pathology. Furthermore, available tau pathology and neurodegeneration biomarkers were consistent with AD: CSF p-tau and t-tau were pathological and FDG-PET voxel-based analyses showed significant hypometabolism in areas typically related to AD, as parieto-temporal lobes, PCC, and precuneus [36].

The triple-negative group showed the opposite scenario, with all available biomarkers in agreement in excluding amyloid pathology due to AD. We have to report that some CSF p-tau and t-tau values were close to cut-offs. Nelson et al. have already observed that brains with medial temporal lobe neurofibrillary tangles but no neuritic amyloid plaques represented a diagnostic dilemma but may have pathogenetic aspects different from AD [37]. In addition to that, medial temporal lobe tau pathology in the absence of β-amyloid is frequently observed at autopsy in cognitively normal individuals, a phenomenon that may reflect a consequence of aging, defined "primary age-related tauopathy," as underlined by A. J. Weigand et al. [38]. However, our triple-negative subjects also presented the highest CSF $A\beta_{42}$ and $A\beta_{42/40}$ mean levels as well as the lowest global SUVR mean value. Moreover, FDG-PET voxel-based analyses did not demonstrate statistically significant hypometabolism in any region as compared to controls.

The remaining part of our sample was represented by discordant cases, whose percentage was about 33%. This outcome is slightly different from other studies, which showed rates of disagreements of around 10–20% [13]. It could be related to the features of our sample, gained from clinical practice rather than from an experimental setting. A similar scenario has been reported in a previous study by Wiese et al., with a discordance rate of 32.5% in a clinical setting [39]. The reason why substantial discordance among these biomarkers can occur represents a still debated field, and explicit guidelines about the interpretation of intraclass biomarker incongruence are currently missing. Several works dealt with this topic, and some of them attributed the disagreement among amyloid biomarkers to the temporal gap existing between CSF $A\beta_{42}$ reduction and Amy-PET alteration [4], highlighting the need to consider AD in terms of a dynamic biological process [6]. On the other hand, starting from the knowledge that CSF $A\beta_{42}$ and Amy-PET reflect

Table 3 *Brain regions showing high significant ^{18}F-labeled amyloid tracers' retention in A(x)R(x)P(x) groups compared to controls (triple-negative subjects).* * *T* and *Z* values are extracted at the peak of maximum significance at $p < 0.05$, correcting for age. Only contrasts yielding significant results are reported. † coordinates (x, y, z) are from Talairach and Tournoux. Abbreviations: *A* cerebrospinal fluid amyloid β 1–42; *R* cerebrospinal fluid amyloid β 1–42/1–40; *P* amyloid positron emission tomography

Cluster extent	T *	Z *	x, y, z †	Anatomical Region	Brodmann Area
A + R + P + > A-R-P-					
4230	10.17	6.20	18, 28, − 21	Right cerebrum, frontal lobe, orbital gyrus, gray matter	47
	9.92	6.13	27, 30, − 17	Right cerebrum, frontal lobe, middle frontal gyrus, gray matter	11
	9.60	6.03	37, 36, − 15	Right cerebrum, frontal lobe, middle frontal gyrus, gray matter	11
3880	9.03	5.85	4, − 42, 31	Right cerebrum, limbic lobe, cingulate gyrus, gray matter	31
	8.43	5.64	− 4, – 54, 31	Left cerebrum, parietal lobe, precuneus, gray matter	31
	8.35	5.61	− 8, − 43, 42	Left cerebrum, limbic lobe, cingulate gyrus, gray matter	31
241	7.97	5.47	− 31, 30, − 16	Left cerebrum, frontal lobe, inferior frontal gyrus, gray matter	47
832	7.87	5.43	− 35, 35, 31	Left cerebrum, frontal lobe, superior frontal gyrus, gray matter	9
	7.80	5.40	− 20, 43, 35	Left cerebrum, frontal lobe, superior frontal gyrus, gray matter	9
	7.34	5.22	− 39, 23, 39	Left cerebrum, frontal lobe, precentral gyrus, gray matter	9
1125	7.51	5.28	− 6, 5, 52	Left cerebrum, frontal lobe, medial frontal gyrus, gray matter	6
	6.98	5.06	0, 41, − 9	Left cerebrum, frontal lobe, medial frontal gyrus, gray matter	11
	6.78	4.98	− 4, 30, 33	Left cerebrum, frontal lobe, medial frontal gyrus, gray matter	9
227	7.44	5.26	57, − 8, 9	Right cerebrum, temporal lobe, superior temporal gyrus, gray matter	22
1866	7.43	5.26	− 59, – 43, 8	Left cerebrum, temporal lobe, superior temporal gyrus, gray matter	22
	7.43	5.25	− 51, − 49, 34	Left cerebrum, parietal lobe, supramarginal gyrus, gray matter	40
	7.35	5.22	− 55, – 57, 1	Left cerebrum, temporal lobe, middle temporal gyrus, gray matter	37
472	7.33	5.21	41, 45, 16	Right cerebrum, frontal lobe, middle frontal gyrus, gray matter	10
	6.71	4.95	25, 43, 32	Right cerebrum, frontal lobe, superior frontal gyrus, gray matter	9
	6.48	4.84	43, 44, 3	Right cerebrum, frontal lobe, inferior frontal gyrus, gray matter	10
230	7.25	5.18	− 29, – 13, − 29	Left cerebrum, limbic lobe, uncus, gray matter	20
	6.47	4.84	− 24, − 17, − 20	Left cerebrum, limbic lobe, parahippocampal gyrus, gray matter	28
	6.23	4.72	− 37, – 16, − 21	Left cerebrum, temporal lobe, sub-gyral, gray matter	20
57	7.22	5.17	− 39, − 41, 45	Left cerebrum, parietal lobe, inferior parietal lobule, gray matter	40
	6.15	4.68	− 31, – 35, 43	Left cerebrum, parietal lobe, inferior parietal lobule, gray matter	40
95	7.05	5.10	− 39, 50, 5	Left cerebrum, frontal lobe, inferior frontal gyrus, gray matter	10
134	7.00	5.07	− 59, – 31, 27	Left cerebrum, parietal lobe, inferior parietal lobule, gray matter	40
93	6.84	5.00	− 55, − 14, 27	Left cerebrum, frontal lobe, precentral gyrus, gray matter	3
61	6.72	4.95	16, 18, − 5	Right cerebrum, sub-lobar, lentiform nucleus, gray matter	Putamen
	6.10	4.66	18, 15, 2	Right cerebrum, sub-lobar, lentiform nucleus, gray matter	Putamen
61	6.69	4.93	51, − 35, 44	Right cerebrum, parietal lobe, inferior parietal lobule, gray matter	40
209	6.68	4.93	49, − 53, -4	Right cerebrum, temporal lobe, inferior temporal gyrus, gray matter	37
	5.88	4.55	61, − 49, 3	Right cerebrum, temporal lobe, middle temporal gyrus, gray matter	21
124	6.68	4.93	31, 57, − 2	Right cerebrum, frontal lobe, superior frontal gyrus, gray matter	10
	6.30	4.76	25, 58, − 7	Right cerebrum, frontal lobe, superior frontal gyrus, gray matter	10
	6.29	4.75	20, 59, − 11	Right cerebrum, frontal lobe, superior frontal gyrus, gray matter	11
309	6.53	4.86	6, 6, 39	Right cerebrum, limbic lobe, cingulate gyrus, gray matter	32
	6.51	4.85	10, 13, 48	Right cerebrum, frontal lobe, superior frontal gyrus, gray matter	6
	6.21	4.71	8, 19, 39	Right cerebrum, limbic lobe, cingulate gyrus, gray matter	32
42	6.44	4.82	− 39, − 39 − 11	Left cerebrum, temporal lobe, fusiform gyrus, gray matter	37
63	6.41	4.81	− 18, 11, − 17	Left cerebrum, frontal lobe, inferior frontal gyrus, gray matter	47
44	6.31	4.76	− 43, − 5, 46	Left cerebrum, frontal lobe, precentral gyrus, gray matter	6
37	6.26	4.73	37, − 71, 29	Right cerebrum, temporal lobe, middle temporal gyrus, gray matter	39
	5.92	4.57	41, − 66, 37	Right cerebrum, parietal lobe, precuneus, gray matter	39
36	6.25	4.73	47, − 62, 26	Right cerebrum, temporal lobe, middle temporal gyrus, gray matter	39

Table 3 (continued)

Cluster extent	T *	Z *	x, y, z †	Anatomical Region	Brodmann Area
22	6.23	4.72	− 14, 17, − 3	Left cerebrum, sub-lobar, caudate, gray matter	Caudate Head
	5.76	4.49	− 8, 11, − 7	Left cerebrum, sub-lobar, gray matter	*
73	6.18	4.70	6, 36, 17	Right cerebrum, limbic lobe, anterior cingulate, gray matter	32
	5.92	4.57	6, 44, 9	Right cerebrum, limbic lobe, anterior cingulate, gray matter	32
22	6.12	4.67	59, − 12, 28	Right cerebrum, frontal lobe, precentral gyrus, gray matter	4
21	6.06	4.64	− 35, − 26, − 15	Left cerebrum, limbic lobe, parahippocampal gyrus, gray matter	36
A-R + P + > A-R-P-					
566	8.06	5.50	25, 36, − 16	Right cerebrum, frontal lobe, middle frontal gyrus, gray matter	11
	7.83	5.41	37, 36, − 16	Right cerebrum, frontal lobe, middle frontal gyrus, gray matter	11
	7.46	5.27	18, 28, − 21	Right cerebrum, frontal lobe, orbital gyrus, gray matter	47
110	7.03	5.09	6, − 44, 33	Right cerebrum, limbic lobe, cingulate gyrus, gray matter	31
25	6.87	5.01	31, 57, 0	Right cerebrum, frontal lobe, middle frontal gyrus, gray matter	*
25	6.61	4.90	16, 19, − 3	Right cerebrum, sub-lobar, caudate, gray matter	Caudate Head
37	6.50	4.85	− 55, − 49, 37	Left cerebrum, parietal lobe, inferior parietal lobule, gray matter	40
17	6.38	4.79	41, 45, 16	Right cerebrum, frontal lobe, middle frontal gyrus, gray matter	10
18	6.36	4.78	− 2, − 21, 34	Left cerebrum, limbic lobe, cingulate gyrus, gray matter	24
22	6.30	4.76	− 61, − 31, 27	Left cerebrum, parietal lobe, inferior parietal lobule, gray matter	40
20	5.98	4.60	− 59, − 30, 1	Left cerebrum, temporal lobe, middle temporal gyrus, gray matter	*

different aspects of amyloid pathology progression, some authors affirmed that the two biomarkers provide partly independent information about AD [14].

Getting into this controversial topic, we set up our study considering simultaneously the data extracted from CSF ($A\beta_{42}$ and R) and PET examination, improving the latter with Amy-PET semiquantitative analysis and the analysis of metabolic pattern at FDG-PET scans. The CSF assay of t-tau and p-tau also supported us in the interpretation of the framework.

Focusing on A + R + P- group, Amy-PET negative results were discordant compared to all CSF available biomarkers. Indeed, not only CSF $A\beta_{42}$ and R were consistent with AD, but also CSF p-tau and t-tau, according to the AD biomarkers profile described by NIA-AA[1]. Moreover, absolute values of CSF $A\beta_{42}$ were enough far from the cut-off to exclude limitations related to its value, with a CSF $A\beta_{42}$ mean value even lower than the triple positive one, although not significantly. Besides, FDG-PET analysis revealed a significant hypometabolism in temporoparietal regions, representing the typical AD pattern [40]. On the other hand, semiquantitative Amy-PET analysis seemed to confirm the correct interpretation of Amy-PET scans at the visual assessment, showing a mean global SUVR significantly lower in these patients as compared to SUVR mean value in Amy-PET positive subjects (A + R + P + and A-R + P +). However, looking at regional SUVR values, the majority of cerebral regions showed an intermediate amyloid load in subjects A + R + P-, lower than triple-positive and A-R + P +, but higher than A + R-P- and triple-negative. Even more interestingly, the semiquantitative analysis demonstrated that in the precuneus A + R + P- SUVR values were the closest to Amy-PET positive subjects ones (A + R + P + and A-R + P +), not showing significant differences compared to A-R + P +. This is in line with the multimodal imaging abnormalities related to AD reported in this region in literature [41]. The precuneus is in fact a cortical area serving in many complex and associated with higher-order cognitive processes [36], well known to be a critical region in the pathological mechanism of AD. Similar results have been found in the posterior cingulate (PCC) and in the dorsolateral inferior cortices, which showed SUVR values not significantly different from A-R + P + and neither from triple positive subjects. The PCC is a highly connected region, with an important cognitive role, and it has been demonstrated that abnormalities in this region could be clearly linked to AD [36]. Furthermore, the precuneus and PCC are known to be part of the default mode network (DMN) and several studies confirmed its specific involvement in the AD early stages [33]. So, precuneus and PCC seem to be promising regions to investigate with semiquantitative analysis to improve Amy-PET Aβ detection in discordant cases. Concerning the relatively high SUVR mean value in the dorsolateral inferior cortex, it is known that frontal lobes are usually spared by AD degeneration until late stages and, consequently, could be relatively spared by atrophy and perfusion reductions [34]. Therefore, the radiotracer could have reached these areas in a large amount and have bound local amyloid deposits without being masked by neurodegeneration phenomena and partial volume effects. This could justify our result and

confirm one more time the crucial role of semiquantitative Amy-PET analysis in terms of diagnostic accuracy for AD, especially in discordant cases CSF + /PET- [21]. In common practice, the possibility to increase the helpful role of semiquantification, by focusing the analysis in specific areas, should be considered. While precuneus and the PCC have been already defined as promising regions in this field [36], the dorsolateral inferior frontal cortex could be taken into account for further investigations.

Moving to the remaining discordant subjects (A + R-P- and A-R + P +), we can interestingly observe that the agreement between R and Amy-PET is respected in both groups, against CSF $A\beta_{42}$ discordant results. This is in line with previous studies showing an agreement between amyloid imaging and AD CSF biomarkers, higher for R than for single CSF $A\beta_{42}$ analyte [16]. Hansson et al., in a recent review, confirmed that CSF $A\beta_{42/40}$ should be used to improve the percentage of appropriately diagnosed patients, overcoming the variability in individual Aβ metabolism [11].

In A + R-P- group, R and Amy-PET negativity is corroborated by T and (N) biomarker, with very low (negative) CSF p-tau mean value, and by the absence of neurodegeneration, showed by negative CSF t-tau and no significant hypometabolism at FDG-PET voxel-based analysis. The overall results led us to hypothesize that CSF $A\beta_{42}$ measurement produced false-positive dichotomic results in our sample. One more interesting datum emerged by the CSF $A\beta_{42}$ assay: $A\beta_{42}$ mean values resulted significantly higher in these subjects than in triple-positive ones, with levels close to the cut-off in absolute terms (mean value − 12% from the threshold). This is in line with the scientific debate about cut-off choices and the consequent uncertain interpretation of cases with $A\beta_{42}$ levels close to it. Therefore, it has been already discussed how discordance occurs mostly in patients with $A\beta_{42}$ measurement close to cut-off [20]. On the whole, we can hypothesize that in discordant subjects with CSF $A\beta_{42}$ levels close to the cut-off, R value could be resolutive.

In A-R + P + group, R and Amy-PET were consistent with AD, as well as CSF p-tau and t-tau (above their cut-offs). The FDG pattern also corroborated the presence of neurodegeneration, showing hypometabolism in PCC [40]. Moreover, brain amyloid deposition is confirmed by Amy-PET semiquantitative evaluations. The SUVR values of these patients were close to the triple-positive ones and significantly higher in this group than in all other Amy-PET negatives subjects (A + R + P-, A + R-P-, A-R-P-), both in global and regional analysis. This is particularly true for AD key regions, such as the parieto-temporal lobes. One more intriguing finding emerged by Amy-PET voxel-based analysis, which showed a significant binding of amyloid tracers in PCC and orbitofrontal cortex. These regions are part of the default mode network, which is known to be early affected by AD [35]. All these findings were therefore consistent with AD and carried us to suppose that the CSF $A\beta_{42}$ evaluation produced false-negative results in this sample. Moreover, the high CSF $A\beta_{42}$ levels, far enough from the adopted threshold, allowed to exclude that CSF $A\beta_{42}$ false-negative results could possibly have been related to cut-off choice. As a result, it appears that R could increase the performance also for patients falsely classified as positive by low CSF $A\beta_{42}$ levels. A possible explanation has been found in the unspecific CSF $A\beta_{42}$ reduction, observed also in other non-AD conditions, including Creutzfeldt-Jakob's disease, amyotrophic lateral sclerosis, neuroinflammation, and other non-AD dementias such as vascular dementia or Parkinson's disease with dementia [19]. The normalization of the CSF $A\beta_{42}$ concentration to the level of the most abundant cerebral Aβ isoform ($A\beta_{1\text{-}40}$), performed by R parameter, could overcome the above-mentioned limitations, being helpful in discordant subjects' interpretation.

By projecting our results into clinical practice, they can be used to clarify when each particular biomarker measurement could be ambiguous. This is true when an amyloid PET scan does not present qualitative and quantitative alterations globally suggestive of AD, but pathological findings are detected in crucial regions (e.g., precuneus, PCC). The suspicion of amyloid pathology should be stronger and further investigations with CSF markers may be appropriate. On the other hand, when CSF marker analysis is available, the discordance between Ab_{42} and ratio seems to be a sufficient parameter to require further investigation by Amy-PET, especially when the absolute value of Ab_{42} is close to the cut-off.

Limitations

This study presents some limitations. We analyzed a relatively small cohort, since Amy-PET is actually considered as an alternative test to CSF analysis and consequently not many cases perform usually both tests. This may lead to reduced statistical power in detecting differences among groups. In order to confirm the study outcomes, a multicenter study or a validation against open-access datasets should be considered. Moreover, the lack of pathological confirmation of diagnosis and the use of different Amy-PET tracers did not allow us to design the study as a test accuracy study. Lastly, CSF cut-offs choice could have influenced agreement between CSF $A\beta_{42}$, $A\beta_{42/40}$, and Amy-PET.

Conclusions

The amyloid discordant cases could be overcome by the combined use of CSF $A\beta_{42}$, CSF $A\beta_{42/40}$, and Amy-PET results as independent parameters. The concordance of any 2

out of the 3 biomarkers seems to support or exclude amyloid pathology, considering the remaining one as a false result.

A cut-off point review could be considered to avoid CSF $A\beta_{42}$ false negatives results.

In discordant cases, the implementation of semiquantitative Amy-PET analyses in support of qualitative interpretation could be useful, and its role might be increased by focusing on regional analysis of specific AD areas, such as precuneus and PCC. Further studies in a larger cohort are warranted to confirm our hypothesis.

Acknowledgements Thanks to Fondazione Turati for providing materials for cerebrospinal fluid assay.

Author contributions Matilde Nerattini: Conceptualization (supporting); writing, original draft preparation (equal); formal analysis (equal); investigation (equal).

Federica Rubino: Conceptualization (supporting); writing, original draft preparation (equal); formal analysis (equal); investigation (equal).

Annachiara ArnoneL Conceptualization (supporting); writing, original draft preparation (equal); formal analysis (equal); investigation (equal).

Cristina Polito: Methodology (equal); writing, review and editing (supporting).

Giulia Puccini: Methodology (equal); writing, review and editing (supporting).

Salvatore Mazzeo: Resources; writing, review and editing (supporting).

Gemma Lombardi: Resources; writing, review and editing (supporting).

Benedetta Nacmias: Resources; writing, review and editing (supporting).

Maria Teresa De Cristofaro: Resources; writing, review and editing (supporting).

Sandro Sorbi: Resources; supervision (supporting); writing, review and editing (supporting).

Alberto Pupi: Writing, review and editing (supporting); supervision (supporting).

Roberto Sciagrà: Writing, review and editing (supporting); supervision (supporting).

Valentina Bessi: Resources; writing, review and editing (supporting).

Valentina Berti: Conceptualization (lead); supervision (lead); writing, original draft (supporting); writing, review and editing (lead).

Declarations

Ethics approval Participants (or their caregivers) gave informed consent for all investigations, and study procedures were approved by the local Institutional Review Board (reference 15691_oss).

Conflict of interest The authors declare that they have no conflicts of interest.

References

1. Jack CR, Bennett DA, Blennow K et al (2018) NIA-AA research framework: toward a biological definition of Alzheimer's disease. Alzheimers Dement 14(4):535–562
2. De Wilde A, Reimand J, Teunissen CE et al (2019) Discordant amyloid-β PET and CSF biomarkers and its clinical consequences. Alzheimers Res Ther 11(1):78 (Published 2019 Sep 12)
3. Blennow K, de Leon MJ, Zetterberg H (2006) Alzheimer's disease. Lancet 368(9533):387–403
4. Palmqvist S, Mattsson N, Hansson O (2016) Cerebrospinal fluid analysis detects cerebral amyloid-β accumulation earlier than positron emission tomography. Brain 139(Pt 4):1226–1236
5. Clark CM, Pontecorvo MJ, Beach TG et al (2012) Cerebral PET with florbetapir compared with neuropathology at autopsy for detection of neuritic amyloid-β plaques: a prospective cohort study. Lancet Neurol. 2012 Aug;11(8):658]. Lancet Neurol 11(8):669–678
6. Sperling RA, Aisen PS, Beckett LA et al (2011) Toward defining the preclinical stages of Alzheimer's disease: recommendations from the National Institute on Aging-Alzheimer's Association workgroups on diagnostic guidelines for Alzheimer's disease. Alzheimers Dement 7(3):280–292
7. Dubois B, Feldman HH, Jacova C et al (2014) Advancing research diagnostic criteria for Alzheimer's disease: the IWG-2 criteria. Lancet Neurol. 13(6):614–629 [published correction appears in Lancet Neurol. 2014 Aug;13(8):757]
8. Albert MS, DeKosky ST, Dickson D et al (2011) The diagnosis of mild cognitive impairment due to Alzheimer's disease: recommendations from the National Institute on Aging-Alzheimer's Association workgroups on diagnostic guidelines for Alzheimer's disease. Alzheimers Dement 7(3):270–279
9. McKhann GM, Knopman DS, Chertkow H et al (2011) The diagnosis of dementia due to Alzheimer's disease: recommendations from the National Institute on Aging-Alzheimer's Association workgroups on diagnostic guidelines for Alzheimer's disease. Alzheimers Dement 7(3):263–269
10. Blennow K, Mattsson N, Schöll M, Hansson O, Zetterberg H (2015) Amyloid biomarkers in Alzheimer's disease. Trends Pharmacol Sci 36(5):297–309
11. Hansson O, Lehmann S, Otto M, Zetterberg H, Lewczuk P (2019) Advantages and disadvantages of the use of the CSF Amyloid β (Aβ) 42/40 ratio in the diagnosis of Alzheimer's Disease. Alzheimers Res Ther 11(1):34 (Published 2019 Apr 22)
12. Mattsson N, Insel PS, Landau S et al (2014) Diagnostic accuracy of CSF Ab42 and florbetapir PET for Alzheimer's disease. Ann Clin Transl Neurol 1(8):534–543
13. Landau SM, Lu M, Joshi AD et al (2013) Comparing positron emission tomography imaging and cerebrospinal fluid measurements of beta-amyloid. AnnNeurol 74(6):826–836
14. Mattsson N, Insel PS, Donohue M et al (2015) Independent information from cerebrospinal fluid amyloid-β and florbetapir imaging in Alzheimer's disease. Brain 138(Pt 3):772–783
15. Wiltfang J, Esselmann H, Bibl M et al (2007) Amyloid β peptide ratio 42/40 but not Aβ42 correlates with phospho-Tau in patients with low- and high-CSF Aβ40 load. J Neurochem 101(4):1053–1059
16. Janelidze S, Zetterberg H, Mattsson N et al (2016) J CSF Aβ42/Aβ40 and Aβ42/Aβ38 ratios: better diagnostic markers of Alzheimer disease. Ann Clin Transl Neurol 3(3):154–165
17. Lewczuk P, Lelental N, Spitzer P, Maler JM, Kornhuber J (2015) Amyloid-β 42/40 cerebrospinal fluid concentration ratio in the diagnostics of Alzheimer's disease: validation of two novel assays. J Alzheimers Dis 43(1):183–191
18. Giacomucci G, Mazzeo S, Bagnoli S et al (2021) Matching clinical diagnosis and amyloid biomarkers in alzheimer's disease and frontotemporal dementia. J Pers Med 11(1):47
19. Augutis K, Axelsson M, Portelius E et al (2013) Cerebrospinal fluid biomarkers of β-amyloid metabolism in multiple sclerosis. Mult Scler 19(5):543–552

20. Zwan M, van Harten A, Ossenkoppele R et al (2014) Concordance between cerebrospinal fluid biomarkers and [11C]PIB PET in a memory clinic cohort. J Alzheimers Dis 41(3):801–807
21. Alongi P, Sardina DS, Coppola R et al (2019) 18F-Florbetaben PET/CT to Assess Alzheimer's Disease: a new analysis method for regional amyloid quantification. J Neuroimaging 29(3):383–393
22. Meyer PF, McSweeney M, Gonneaud J, Villeneuve S (2019) AD molecular: PET amyloid imaging across the Alzheimer's disease spectrum: from disease mechanisms to prevention. Prog Mol Biol Transl Sci 165:63–106
23. Lombardi G, Pupi A, Bessi V et al (2020) Challenges in Alzheimer's disease diagnostic work-up: amyloid biomarker incongruences. J Alzheimers Dis 77(1):203–217
24. Fazekas F, Chawluk JB, Alavi A, Hurtig HI, Zimmerman RA (1987) MR signal abnormalities at 1.5 T in Alzheimer's dementia and normal aging. AJR Am J Roentgenol 149(2):351–356
25. Rudilosso S, San Román L, Blasco J, Hernández-Pérez M, Urra X, Chamorro Á (2017) Evaluation of white matter hypodensities on computed tomography in stroke patients using the Fazekas score. Clin Imaging 46:24–27
26. Kollhoff AL, Howell JC, Hu WT (2018) Automation vs experience: measuring Alzheimer's beta-amyloid 1–42 peptide in the CSF. Front Aging Neurosci 10:253 (Published 2018 Aug 22)
27. Friston KJ, Holmes AP, Worsley KJ, Poline J-P, Frith CD, Frackowiak RSJ (1994) Statistical parametric maps in functional imaging: a general linear approach. Hum Brain Mapp 2(4):189–210
28. Della Rosa PA, Cerami C, Gallivanone F et al (2014) A standardized [18F]-FDG-PET template for spatial normalization in statistical parametric mapping of dementia. Neuroinformatics 12(4):575–593
29. Perani D, Della Rosa PA, Cerami C et al (2014) Validation of an optimized SPM procedure for FDG-PET in dementia diagnosis in a clinical setting. NeuroImage Clin 2014(6):445–454
30. Rolls ET, Huang CC, Lin CP, Feng J, Joliot M (2020) Automated anatomical labelling atlas 3. Neuroimage. 206:116189
31. Palmqvist S, Zetterberg H, Mattsson N et al (2015) Detailed comparison of amyloid PET and CSF biomarkers for identifying early Alzheimer disease. Neurology 85(14):1240–1249
32. Nobili F, Arbizu J, Bouwman F et al (2018) European Association of Nuclear Medicine and European Academy of Neurology recommendations for the use of brain ^{18} F-fluorodeoxyglucose positron emission tomography in neurodegenerative cognitive impairment and dementia: Delphi consensus. Eur J Neurol 25(10):1201–1217
33. Fodero-Tavoletti MT, Cappai R, McLean CA et al (2009) Amyloid imaging in Alzheimer's disease and other dementias. Brain Imaging Behav 3(3):246–261
34. Braak H, Braak E (1991) Neuropathological stageing of Alzheimer-related changes. Acta Neuropathol 82(4):239–259
35. Palmqvist S, Schöll M, Strandberg O et al (2017) Earliest accumulation of β-amyloid occurs within the default-mode network and concurrently affects brain connectivity. Nat Commun 8(1):1214
36. Berti V, Pupi A, Mosconi L (2011) PET/CT in diagnosis of dementia. Ann N Y Acad Sci 1228:81–92
37. Nelson PT, Abner EL, Schmitt FA et al (2009) Brains with medial temporal lobe neurofibrillary tangles but no neuritic amyloid plaques are a diagnostic dilemma but may have pathogenetic aspects distinct from alzheimer disease. J Neuropathol Exp Neurol 68(7):774–784
38. Weigand AJ, Bangen KJ, Thomas KR et al (2020) Is tau in the absence of amyloid on the Alzheimer's continuum?: A study of discordant PET positivity. Brain Commun 2(1):fcz046
39. Weise D, Tiepolt S, Awissus C et al (2015) Critical Comparison of Different Biomarkers for Alzheimer's Disease in a Clinical Setting. J Alzheimers Dis 48(2):425–432
40. Herholz K, Salmon E, Perani D et al (2002) Discrimination between Alzheimer dementia and controls by automated analysis of multicenter FDG PET. Neuroimage 17(1):302–316
41. Karas G, Scheltens P, Rombouts S et al (2007) Precuneus atrophy in early-onset Alzheimer's disease: A morphometric structural MRI study. Neuroradiology 49(12):967–976